

Cobalt-Centered Ten-Vertex Germanium Clusters: The Pentagonal Prism as an Alternative to Polyhedra Predicted by the Wade–Mingos Rules

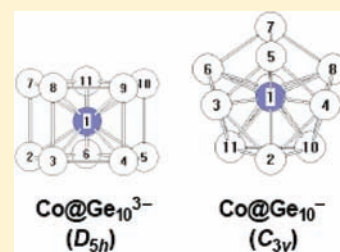
M. M. Uță,[†] D. Cioloboc,[†] and R. B. King^{*,‡}

[†]Faculty of Chemistry and Chemical Engineering, Babeş-Bolyai University, Cluj-Napoca, Romania

[‡]Department of Chemistry, University of Georgia, Athens, Georgia 30602, United States

Supporting Information

ABSTRACT: One of the most exciting recent (2009) discoveries in metal cluster chemistry is the pentagonal prismatic Co@Ge_{10}^{3-} ion, found in $[\text{K}(2,2,2\text{-crypt})]_4[\text{Co@Ge}_{10}][\text{Co}(1,5\text{-C}_8\text{H}_{12})_2] \cdot \text{toluene}$ and characterized structurally by X-ray diffraction. The complete absence of triangular faces in the pentagonal prismatic structure of Co@Ge_{10}^{3-} contradicts expectations from the well-established Wade–Mingos rules, which predict polyhedral structures having mainly or entirely triangular faces. A theoretical study on Co@Ge_{10}^z systems ($z = -5$ to $+1$) predicts a singlet D_{5h} pentagonal prismatic global minimum for the trianion Co@Ge_{10}^{3-} in accord with this experimental result. Redox reactions on this pentagonal prismatic Co@Ge_{10}^{3-} trianion generate low-energy pentagonal prismatic structures for Co@Ge_{10}^z where $z = 0, -1, -2, -4,$ and -5 having quartet, triplet, doublet, doublet, and triplet spin states, respectively. Similar theoretical methods predict a singlet C_{3v} polyhedral structure for the monoanion Co@Ge_{10}^{-} , similar to previous theoretical predictions on the isoelectronic neutral Ni@Ge_{10} and the structure realized experimentally in the isoelectronic Ni@In_{10}^{10-} found in the $\text{K}_{10}\text{In}_{10}\text{Ni}$ intermetallic. Redox reactions on this C_{3v} polyhedral Co@Ge_{10}^{-} monoanion generate low energy C_{3v} polyhedral structures for Co@Ge_{10}^z where $z = 0, -2, -3,$ and -4 having doublet, doublet, triplet, and quartet spin states, respectively.



1. INTRODUCTION

Modern work on bare post-transition element clusters dates back to the 1960s after Corbett and co-workers found ways to obtain crystalline derivatives by use of suitable counterions.^{1,2} This provided for the first time the possibility of definitive elucidation of the structures of such clusters using X-ray crystallography. Such crystalline derivatives of the cluster anions had cryptate or polyamine complexed alkali metals as counterions.¹ Similarly, crystalline derivatives of the cluster cations had counteranions, such as AlCl_4^- , derived from metal halide strong Lewis acids.²

The information arising from the early structural studies of such clusters suggested an analogy with the polyhedral boranes, the chemistry of which was developing concurrently. The borane dianions $\text{B}_n\text{H}_n^{2-}$ and isoelectronic carboranes $\text{C}_2\text{B}_{n-2}\text{H}_n$ having $2n + 2$ skeletal electrons ($6 \leq n \leq 12$) were found to exhibit structures based on deltahedra, that is, polyhedra with all triangular faces. The rules correlating shape of polyhedral boranes with the skeletal electron count were first observed by Williams³ and developed further by Wade^{4,5} and then Mingos.^{6,7} They have subsequently become known as the Wade–Mingos rules.

The Wade–Mingos rules^{4–7} have been applied not only to polyhedral boranes and carboranes but also to metal clusters of various types, including bare post-transition metal clusters. However, limitations in the applications of the Wade–Mingos rules to rationalize the structures of such clusters have become increasingly apparent as these rules were applied to an increasing

variety of systems. For example, the icosahedral borane $\text{B}_{12}\text{H}_{12}^{2-}$ as well as the isoelectronic carboranes $\text{CB}_{11}\text{H}_{12}^-$ and $\text{C}_2\text{B}_{10}\text{H}_{12}$ are all very stable species as predicted by the Wade–Mingos rules for n -vertex clusters having $2n + 2$ skeletal electrons. However, the isoelectronic icosahedral bare group 14 element clusters E_{12}^{2-} ($\text{E} = \text{Si}, \text{Ge},$ and Sn) remain essentially unknown. In this case the Nucleus Independent Chemical Shifts (NICS) test for aromaticity developed by Schleyer and collaborators⁸ provides an explanation for this anomaly. Thus using the NICS test, $\text{B}_{12}\text{H}_{12}^{2-}$ is found to be aromatic but the isoelectronic and still unknown Si_{12}^{2-} is found to be antiaromatic.⁹ Furthermore, for the bare icosahedral clusters E_{12}^{2-} ($\text{E} = \text{Si}, \text{Ge}, \text{Sn}, \text{Pb}$), descending the group 14 column of the Periodic Table increases the aromaticity so that the icosahedral lead cluster Pb_{12}^{2-} is found to be aromatic.¹⁰

The Wade–Mingos rules^{4–7} predict cluster structures based on deltahedra with only triangular faces for systems having $2n + 2$ skeletal electrons. The predicted polyhedra for electron-rich clusters with n vertices having more than $2n + 2$ skeletal electrons may have one or more nontriangular faces but most of the faces are still triangles. Thus it was a real surprise when the Ge_{10} polyhedra in the ten-vertex clusters M@Ge_{10}^{3-} ($\text{M} = \text{Co},^{11} \text{Fe}^{12}$) were recently (2009) found to be pentagonal prisms with no triangular faces at all!

Received: October 13, 2011

Published: March 5, 2012

To understand the nature of these very unusual transition metal-centered pentagonal prismatic 10-vertex clusters, the properties of both the interstitial transition metal atom and the surrounding 10-vertex polyhedron need to be considered. Metal clusters containing interstitial transition metal atoms predate the discovery of bare post-transition element clusters with such interstitial atoms by several years. A particularly informative cluster is the icosahedral nickel carbonyl cluster $\text{Ni}@\text{Ni}_{10}[\text{Sb} \rightarrow \text{Ni}(\text{CO})_3]_2(\text{CO})_{18}^{4-}$, first synthesized by Longoni and co-workers in 1990.¹³ Electron bookkeeping in this cluster counting $\text{Ni}(\text{CO})_2$ vertices as donors of two skeletal electrons like BH vertices in carboranes and $\text{Sb} \rightarrow \text{Ni}(\text{CO})_3$ vertices as donors of three skeletal electrons like CH vertices in carboranes suggests that the interstitial nickel atom is a donor of zero skeletal electrons. This is not unreasonable because a neutral nickel atom has a filled d^{10} shell.¹⁴ By analogy the interstitial neutral d^9 cobalt atom in $\text{Co}@\text{Ge}_{10}^{3-}$ requires one electron to attain a similar filled d^{10} shell and thus can be considered to be a one-electron acceptor or, alternatively stated, a -1 electron donor. Thus $\text{Co}@\text{Ge}_{10}^{3-}$ becomes isoelectronic with the $2n + 2$ skeletal electron ten-vertex system Ge_{10}^{2-} . Density functional theory¹⁵ as well as the Wade–Mingos rules^{4–7} predicts a D_{4d} bicapped square antiprism structure for Ge_{10}^{2-} and thus, by isoelectronic analogy, also for $\text{Co}@\text{Ge}_{10}^{3-}$. Thus the experimental observation of a pentagonal prism rather than a bicapped square antiprism structure for $\text{Co}@\text{Ge}_{10}^{3-}$ is another example of the limitations of the Wade–Mingos rules. The observation of a pentagonal prismatic structure for $\text{Co}@\text{Ge}_{10}^{3-}$ rather than the bicapped square antiprismatic structure predicted by the Wade–Mingos rules may relate to the larger volume of the pentagonal prism, which thus can more readily accommodate the interstitial cobalt atom.

The experimental report of a pentagonal prismatic rather than a bicapped square antiprismatic structure for $\text{Co}@\text{Ge}_{10}^{3-}$ was accompanied by some theoretical studies on $\text{Co}@\text{Ge}_{10}^{3-}$ as well as the isoelectronic $\text{Ni}@\text{Ge}_{10}^{2-}$ and the empty Ge_{10}^{2-} cluster.¹¹ These studies indicate that the D_{5h} pentagonal prism is the ground state structure for $\text{Co}@\text{Ge}_{10}^{3-}$ in accord with the experimental work. However, both these theoretical studies and other concurrently published theoretical studies¹⁶ indicate the D_{4d} bicapped square antiprism to be the ground state for both $\text{Ni}@\text{Ge}_{10}^{2-}$ and the empty Ge_{10}^{2-} . The D_{5h} pentagonal prism structure for $\text{Ni}@\text{Ge}_{10}^{2-}$ is found to lie only ~ 6 kcal/mol above the global minimum.

Binary Co/Ge clusters have also been observed in the gas phase in laser vaporization experiments.^{17,18} The monoanion CoGe_{10}^- exhibited a particularly strong peak in the mass spectra from such experiments. An endohedral $\text{Co}@\text{Ge}_{10}^-$ structure was suggested for this species.

In addition to the unexpected observation of pentagonal prismatic structures for the $\text{M}@\text{Ge}_{10}^{3-}$ clusters ($\text{M} = \text{Fe},^{12} \text{Co}^{11}$), the ten-vertex post-transition element clusters are of interest because of the variety of polyhedra of distinctive symmetries that have been found experimentally by X-ray crystallography in cluster structures containing interstitial atoms (Figure 1). The D_{4d} bicapped square antiprism is found to encapsulate a post-transition metal atom in the anionic indium cluster $\text{Zn}@\text{In}_{10}^{8-}$ found in the intermetallic¹⁹ $\text{K}_8\text{In}_{10}\text{Zn}$ as well as the lead clusters $\text{M}@\text{Pb}_{10}^{2-}$ in $[\text{K}(2,2,2\text{-crypt})]_2[\text{M}@\text{Pb}_{10}]$ ($\text{M} = \text{Ni}, \text{Pd}, \text{Pt}$).^{20,21} A C_{3v} tetracapped trigonal prism is found in the $\text{M}@\text{In}_{10}^{10-}$ clusters found in the $\text{K}_{10}\text{In}_{10}\text{M}$ intermetallics ($\text{M} = \text{Ni}, \text{Pd}, \text{Pt}$), isoelectronic with $\text{Zn}@\text{In}_{10}^{8-}$.²² A pentagonal antiprism of bismuth atoms is the host polyhedron for an interstitial

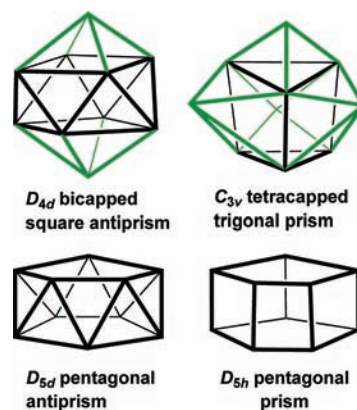


Figure 1. Four ten-vertex polyhedra found as host polyhedra for interstitial metal atoms. For clarity the edges of capping vertices are shown in green.

palladium atom in the cationic bismuth cluster $\text{Pd}@\text{Bi}_{10}^{4+}$ in $\text{Bi}_{14}\text{PdBr}_{16}$ ($= [\text{Pd}@\text{Bi}_{10}][\text{BiBr}_4]_4$).²³

The surprising pentagonal prismatic geometry realized experimentally in $\text{Co}@\text{Ge}_{10}^{3-}$ makes of interest the theoretical study of a wide range of cobalt-centered 10-vertex germanium clusters having various numbers of skeletal electrons. This paper reports a density functional theory study of the cobalt-centered ten-vertex germanium clusters $\text{Co}@\text{Ge}_{10}^z$ with charges ranging from $z = -5$ to $+1$. If the interstitial cobalt atom is considered to be a -1 electron donor (i.e., an acceptor of a single electron), then these systems have from 24 to 18 skeletal electrons. These $\text{Co}@\text{Ge}_{10}^z$ systems includes not only the trianion $\text{Co}@\text{Ge}_{10}^{3-}$, shown experimentally¹¹ to have pentagonal prismatic geometry, but also the monoanion $\text{Co}@\text{Ge}_{10}^-$ observed in the gas phase in laser vaporization experiments^{17,18} and isoelectronic with $\text{Ni}@\text{In}_{10}^{10-}$ and $\text{Zn}@\text{In}_{10}^{8-}$ found in the intermetallics $\text{K}_{10}\text{In}_{10}\text{Ni}$ ²² and $\text{K}_8\text{In}_{10}\text{Zn}$,¹⁹ respectively. The current paper thus extends significantly the theoretical studies limited to the D_{5h} , D_{5d} , and D_{4d} structures of $\text{Co}@\text{Ge}_{10}^{3-}$ and the essentially isoelectronic $\text{Ni}@\text{Ge}_{10}^{2-}$ and Ge_{10}^{2-} included in the original report by Fässler and collaborators¹¹ on the synthesis and structural characterization of $\text{Co}@\text{Ge}_{10}^{3-}$. In particular, the earlier authors did not consider $\text{Co}@\text{Ge}_{10}^z$ species having charges other than -3 nor any possible structures with 3-fold symmetry, such as C_{3v} . We find C_{3v} structures to be low energy structures for many of the $\text{Co}@\text{Ge}_{10}^z$ species, including particularly singlet $\text{Co}@\text{Ge}_{10}^-$.

2. THEORETICAL METHODS

Geometry optimizations were carried out at the hybrid DFT B3LYP level^{24–27} with the 6-31G(d) (valence) double- ζ quality basis functions extended by adding one set of polarization (d) functions for both the interstitial and germanium atoms. The Gaussian 09 package of programs²⁸ was used in which the fine grid (75,302) is the default for numerically evaluating the integrals and the tight (10^{-8}) hartree stands as default for the self-consistent field convergence. Computations were carried out using six initial geometries including ten-vertex polyhedra with 3-fold, 4-fold, and 5-fold symmetry including the four polyhedra in Figure 1 as well as a prolate C_{3v} structure and the D_{4h} bicapped cube. The symmetries were maintained during the initial geometry optimization processes. Symmetry breaking using modes defined by imaginary vibrational frequencies was then used to determine optimized structures with minimum energies. Spin states from singlets to quintets were considered. Vibrational analyses show that all of the final optimized structures discussed in this paper are genuine minima at the B3LYP/6-31G(d) level without any significant imaginary frequencies

($N_{\text{imag}} = 0$). In a few cases the calculations ended with acceptable small imaginary frequencies²⁹ and these values are indicated in the corresponding figures.

The optimized structures found for the Co@Ge_{10}^z derivatives are labeled by the number of skeletal electrons and their relative energies. In determining the numbers of skeletal electrons the interstitial cobalt atom is assumed to attain the d^{10} closed-shell configuration by being a one-electron acceptor, that is, a -1 skeletal electron donor. The germanium vertices are assumed to be donors of two skeletal electrons each as suggested by the Wade–Mingos rules.^{4–7} Spin states are indicated by S, D, T, Q, and P for singlet, doublet, triplet, quartet, and quintet, respectively. Thus the lowest energy structure of the singlet trianion Co@Ge_{10}^{3-} is labeled 22–1S. Additional details of all of the optimized structures, including all interatomic distances, the initial geometries leading to a given optimized structure, and structures with energies too high to be of possible chemical relevance are provided in the Supporting Information. Only structures within 25 kcal/mol of the global minima are considered. In assigning polyhedra to the optimized structures, the Ge–Ge distances less than ~ 3.2 Å were normally considered as polyhedral edges; significant exceptions are noted in the text. Similarly Co–Ge distances less than ~ 2.8 Å are considered bonding distances; most such CoGe bonding distances were less than ~ 2.5 Å except for those some of the less regular polyhedral structures.

3. RESULTS

3.1. Neutral Co@Ge_{10} . Three structures were found for the neutral Co@Ge_{10} within 25 kcal/mol of the global minimum (Figure 2). The global minimum is a doublet C_{3v} structure

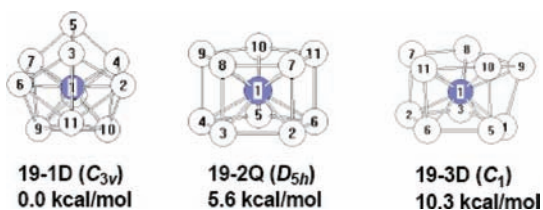


Figure 2. Three structures for the neutral Co@Ge_{10} within 25 kcal/mol of the global minimum.

19–1D. A quartet pentagonal prismatic structure 19–2Q lies 5.6 kcal/mol above this global minimum. A doublet distorted pentagonal prismatic structure 19–3D is also found at 10.3 kcal/mol above 19–1D.

3.2. Anionic Co@Ge_{10}^z Derivatives ($z = -1$ to -5). Four structures were found for the monoanion Co@Ge_{10}^{-} within 25 kcal/mol of the global minimum (Figure 3). The lowest energy

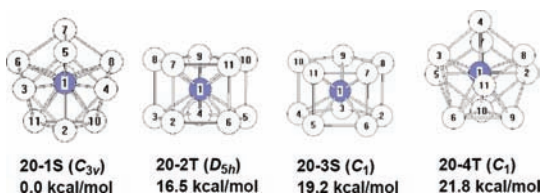


Figure 3. Four structures for the monoanion Co@Ge_{10}^{-} within 25 kcal/mol of the global minimum.

structure is the singlet C_{3v} structure 20–1S based on a polyhedron similar to the isoelectronic In_{10}^{10-} polyhedron found experimentally²² in the intermetallic $\text{K}_{10}\text{In}_{10}\text{Ni}$ and also predicted theoretically¹⁶ for the likewise isoelectronic neutral Ni@Ge_{10} . The next highest energy Co@Ge_{10}^{-} structure is the triplet D_{5h} pentagonal prismatic structure 20–2T, already lying 16.5 kcal/mol above 20–1S. The large energy difference between 20–1S and 20–2T suggests that 20–1S is a highly

favorable structure. Two higher energy distorted Co@Ge_{10}^{-} structures are also found, namely, singlet 20–3S, lying 19.2 kcal/mol above 20–1S and derived from a pentagonal prism, and triplet 20–4T, lying 21.8 kcal/mol above 20–1S.

Three structures were found for the dianion Co@Ge_{10}^{2-} within 25 kcal/mol of the global minimum (Figure 4). The

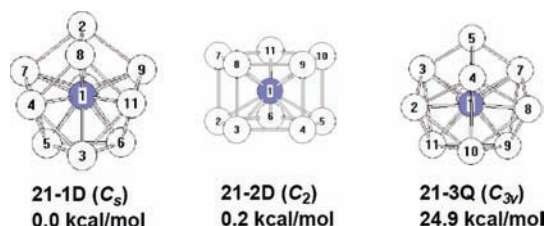


Figure 4. Three structures for the dianion Co@Ge_{10}^{2-} within 25 kcal/mol of the global minimum.

lowest energy structure by only 0.2 kcal/mol is the doublet C_s structure 21–1D with a polyhedron similar to the 20–1S global minimum of the monoanion Co@Ge_{10}^{-} (Figure 3). The doublet dianion structure 21–2D is a slightly distorted pentagonal prism lying only 0.2 kcal/mol above 21–1D (Figure 4). A C_{3v} quartet structure 21–3Q for the dianion Co@Ge_{10}^{2-} lies at a considerably higher energy, namely, 24.9 kcal/mol above 21–1D.

Three structures were found for the trianion Co@Ge_{10}^{3-} within 25 kcal/mol of the global minimum 22–1S (Figure 5).

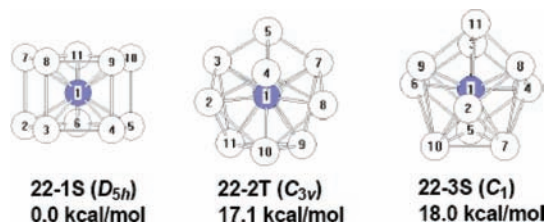


Figure 5. Three structures for the trianion Co@Ge_{10}^{3-} within 25 kcal/mol of the global minimum.

The singlet spin state pentagonal prism Co@Ge_{10}^{3-} structure 22–1S is found experimentally in $[\text{K}(2,2,2\text{-crypt})]_4[\text{Co@Ge}_{10}][\text{Co}(1,5\text{-C}_8\text{H}_{12})_2]\cdot\text{toluene}$ ¹¹ and lies ~ 17 kcal/mol in energy below any other of the Co@Ge_{10}^{3-} structures. The predicted length of the “vertical” edges of the pentagonal prism in 22–1S is 2.59 Å as compared with the experimental value of 2.66 Å. Similarly, the predicted length of the “horizontal” edges of the pentagonal prism in 22–1S (i.e., the edges of the pentagonal faces) is 2.50 Å as compared with the experimental value of 2.51 Å.

The next Co@Ge_{10}^{3-} structure in terms of energy, namely, the triplet structure 22–2T, lies ~ 17 kcal/mol above the pentagonal prism global minimum 22–1S suggesting that the experimentally observed 22–1S is a highly favored structure. Structure 22–2T (Figure 5) is a triplet spin state C_{3v} polyhedron similar to the polyhedra in the singlet 20–1S monoanion global minimum (Figure 3) and the doublet Co@Ge_{10}^{2-} dianion global minimum structure 21–1D (Figure 4). A distorted C_{3v} singlet structure for the Co@Ge_{10}^{3-} trianion 22–3S is also found at 18.0 kcal/mol above the global minimum 22–1S, similar to the triplet monoanion structure 20–4T (Figure 3).

Four structures were found for the tetraanion Co@Ge_{10}^{4-} within 25 kcal/mol of the global minimum (Figure 6). The

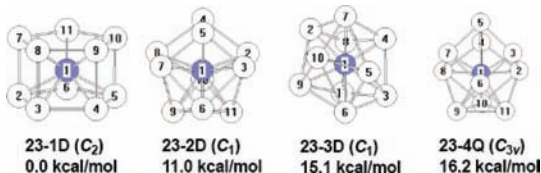


Figure 6. Four structures for the tetraanion Co@Ge_{10}^{4-} within 25 kcal/mol of the global minimum.

lowest energy of these structures, namely, doublet **23-1D**, is a slightly distorted pentagonal prism. This structure is reasonably favorable since the next Co@Ge_{10}^{4-} structure, namely, doublet **23-2D**, lies 11 kcal/mol above **23-1D**. Structure **23-2D** is a slightly distorted C_{3v} polyhedron similar to the C_{3v} polyhedron found in singlet **22-3S**.

The next Co@Ge_{10}^{4-} tetraanion structure in terms of energy, namely **23-3D** at 15.1 kcal/mol above **23-1D** (Figure 6), is derived from the D_{4d} bicapped square antiprism but is so highly distorted that its origin is hardly recognizable. This suggests that the cavity in a bicapped square antiprism, or actually that in the underlying square antiprism, is not large enough to accommodate an interstitial cobalt atom.

The lowest lying quartet structure for the Co@Ge_{10}^{4-} tetraanion, namely, **23-4Q** at 16.2 kcal/mol in energy above **23-1D** (Figure 6), is an undistorted C_{3v} polyhedron similar to the C_{3v} polyhedron found in the global minima for the Co@Ge_{10}^{-} monoanion (singlet **20-1S** in Figure 3) and the Co@Ge_{10}^{2-} dianion (doublet **21-1D** in Figure 4).

The potential energy surface of the Co@Ge_{10}^{5-} pentaanion is more complicated since eight structures are found within 25 kcal/mol of the global minimum **24-1T** (Figure 7). These

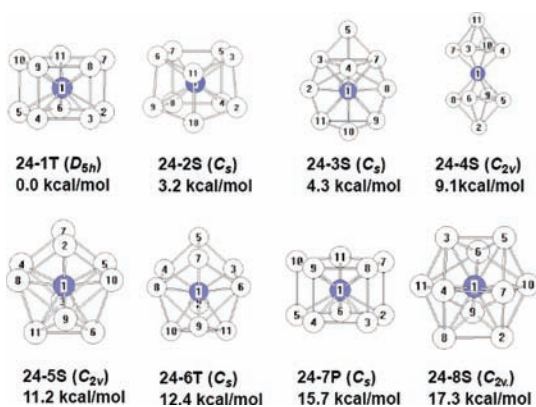


Figure 7. Eight structures for the pentaanion Co@Ge_{10}^{5-} within 25 kcal/mol of the global minimum.

eight structures include five singlet structures, two triplet structures, and a single quintet structure.

The lowest energy Co@Ge_{10}^{5-} structure is the D_{5h} triplet pentagonal prism **24-1T** (Figure 7). The other triplet Co@Ge_{10}^{5-} structure is the C_s polyhedral structure **24-6T** lying 12.4 kcal/mol above **24-1T**. The Ge_{10} polyhedron in **24-6T** is a relatively open polyhedron with six quadrilateral faces and four triangular faces corresponding to six degree 4 vertices and four degree 3 vertices. The lone quintet Co@Ge_{10}^{5-} structure

24-7P, lying 15.7 kcal/mol above **24-1T**, is a distorted pentagonal prism.

The five singlet Co@Ge_{10}^{5-} structures are all distorted from ideal polyhedra (Figure 7). The lowest energy singlet structure **24-2S** lies 3.2 kcal/mol above the global minimum **24-1T** and is a distorted pentagonal prism. The next singlet Co@Ge_{10}^{5-} structure **24-3S** lies 4.3 kcal/mol above **24-1T**. Structure **24-3S** is derived from a C_{3v} polyhedron distorted to C_s symmetry. In the singlet structure **24-4S**, lying 9.1 kcal/mol above **24-1T**, the Ge_{10} polyhedron has split into two Ge_5 units. Thus structure **24-4S** can be considered to be two octahedra sharing a vertex. The shared vertex is the cobalt atom. The singlet Co@Ge_{10}^{5-} structure **24-5S**, lying 11.2 kcal/mol above **24-1S**, has a C_{2v} Ge_{10} polyhedron very similar to the C_s Ge_{10} polyhedron in the triplet structure **24-6T** discussed above. The highest energy singlet Co@Ge_{10}^{5-} structure, namely, **24-8S** lying 17.3 kcal/mol above **24-1T**, has a C_{2v} Ge_{10} polyhedron which is more closed than that in **24-5S**. The Ge_{10} polyhedron in **24-8S** has two quadrilateral faces and 12 triangular faces corresponding to four degree 5 vertices and six degree 4 vertices.

3.3. Cation Co@Ge_{10}^+ . Four structures were found for the Co@Ge_{10}^+ cation within 25 kcal/mol of the global minimum (Figure 8). The lowest energy Co@Ge_{10}^+ structure is the

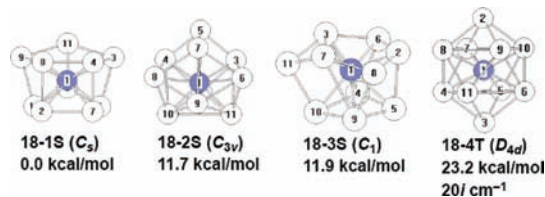


Figure 8. Four structures for the cation Co@Ge_{10}^+ within 25 kcal/mol of the global minimum.

singlet C_s distorted pentagonal prism **18-1S**. The next Co@Ge_{10}^+ structure is the singlet C_{3v} polyhedral structure **18-2S**, lying 11.7 kcal/mol above **18-1S**. The final singlet Co@Ge_{10}^+ structure is the highly distorted polyhedral structure **18-3S**, lying 11.9 kcal/mol above **18-1S**. A single triplet structure, namely, the D_{4d} bicapped square antiprismatic structure **18-4T**, was found at 23.2 kcal/mol above **18-1S** with a small imaginary vibrational frequency at $20i \text{ cm}^{-1}$. Structure **18-4T** is the only Co@Ge_{10}^z ($z = -5$ to $+1$) structure found based on this D_{4d} deltahedron within 25 kcal/mol of a global minimum.

4. DISCUSSION

Four 10-vertex polyhedra, namely, the D_{4d} bicapped square antiprism, the C_{3v} tetracapped trigonal prism, the D_{5d} pentagonal antiprism, and the D_{5h} pentagonal prism (Figure 1), have been found in centered 10-vertex clusters that have been synthesized and structurally characterized by X-ray crystallography. Among these four polyhedra only the tetracapped trigonal prism and pentagonal prism are found in undistorted form in several of the low-energy Co@Ge_{10}^z structures ($z = -5$ to $+1$). The bicapped square antiprism is found only in the relatively high energy triplet Co@Ge_{10}^+ structure **18-4T** (Figure 8). No low energy Co@Ge_{10}^z structures with pentagonal antiprismatic geometry were found. In general attempted optimizations of Co@Ge_{10}^z structures of various spin multiplicities starting with polyhedra other than the tetracapped trigonal prism and pentagonal prism lead to structures at very high energies, highly distorted low energy

structures, or structures with pentagonal prismatic or tetracapped trigonal prismatic geometry.

A singlet pentagonal prismatic structure **22–1S** (Figure 5) was found to be the global minimum for the trianion Co@Ge_{10}^{3-} in accord with the observation of this structure by X-ray crystallography in $[\text{K}(2,2,2\text{-crypt})]_4[\text{Co@Ge}_{10}][\text{Co}(1,5\text{-C}_8\text{H}_{12})_2]\cdot\text{toluene}$.¹¹ This structure is obviously a very favorable “closed shell” structure since it lies ~ 17 kcal/mol in energy below the next lowest energy Co@Ge_{10}^{3-} structure, namely, the triplet **22–2T** (Figure 5). Addition of an electron to the Co@Ge_{10}^{3-} structure **22–1S** gives the doublet pentagonal prismatic structure **23–1D** for Co@Ge_{10}^{4-} (Figure 6). This structure can be considered formally as a radical tetraanion. Further addition of an electron to the tetraanion **23–1D** gives the triplet pentaanion Co@Ge_{10}^{5-} structure **24–1T** (Figure 7). Both **23–1D** and **24–1T** are global minima indicating the generally high stability of pentagonal prismatic Co@Ge_{10}^z structures.

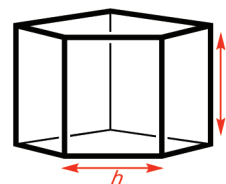
Higher spin state pentagonal prismatic Co@Ge_{10}^z structures can also be obtained by removal of electrons from the singlet stable trianion Co@Ge_{10}^{3-} structure **22–1S** (Figure 5). Thus removal of one electron from **22–1S** gives the doublet Co@Ge_{10}^{2-} dianion pentagonal prismatic structure **21–2D**, which lies within 0.2 kcal/mol of the global minimum. The doublet pentagonal prismatic structure **21–2D** for the dianion Co@Ge_{10}^{2-} is isoelectronic with the known pentagonal prismatic iron-centered ten-vertex germanium polyhedral anion Fe@Ge_{10}^{3-} , which has been synthesized and characterized by X-ray crystallography.¹² Further successive removal of electrons from the Co@Ge_{10}^{2-} dianion structure **21–2D** gives successively low-energy pentagonal prismatic structures for the Co@Ge_{10}^- anion (triplet **20–2T** in Figure 3) and for neutral Co@Ge_{10} (quartet **19–2Q** in Figure 2). The latter two structures are not global minima but lie relatively close to C_{3v} tetracapped trigonal prismatic global minima. The existence of low energy pentagonal prismatic Co@Ge_{10}^z structures for the six charges (z) from 0 to -5 suggests that the redox chemistry of the known Co@Ge_{10}^{3-} is likely to be very rich. However, meaningful electrochemical studies of Co@Ge_{10}^{3-} would probably require generation of this trianion in the absence of other potentially redox active species. Thus, electrochemical studies on the known derivative $[\text{K}(2,2,2\text{-crypt})]_4[\text{Co@Ge}_{10}][\text{Co}(1,5\text{-C}_8\text{H}_{12})_2]\cdot\text{toluene}$ are likely to be complicated by the redox chemistry of the $\text{Co}(1,5\text{-C}_8\text{H}_{12})_2^-$ anion also present in this derivative.

A central question in this work is why the D_{5h} pentagonal prism structure is strongly preferred over the D_{4d} bicapped square antiprism structure for Co@Ge_{10}^{3-} . Thus the species Co@Ge_{10}^{3-} has 22 skeletal electrons if the interstitial cobalt atom is considered to be a -1 electron donor (i.e., an one-electron acceptor). The Wade–Mingos rules^{4–7} would suggest a D_{4d} bicapped square antiprism structure for Co@Ge_{10}^{3-} similar to the experimental structure for $\text{B}_{10}\text{H}_{10}^{2-}$ or structures predicted theoretically for Ge_{10}^{2-} and Ni@Ge_{10}^{2-} . However, the internal volume of a polyhedron having a given number of vertices is maximized by minimizing the number of polyhedral edges. For example, polyhedra having all degree 3 vertices, such as the prisms, maximize the internal volumes for a given even number of vertices. We suggest that the larger internal volume of a pentagonal prism relative to a bicapped square antiprism makes the pentagonal prism the preferred Ge_{10} polyhedron to encapsulate a cobalt atom in a 22 skeletal electron system. This suggestion is supported by our previous theoretical studies¹⁶ on

the related 22 skeletal electron systems M@Ge_{10}^{2-} ($\text{M} = \text{Ni}, \text{Pd}, \text{Pt}$). These theoretical studies were completed and submitted for publication before the first experimental publication on Co@Ge_{10}^{3-} in 2009.¹¹ For the nickel derivative the D_{4d} bicapped square antiprism is found to be the global minimum with the D_{5h} Ni@Ge_{10}^{2-} pentagonal prism lying only 5.7 kcal/mol above this global minimum. This result is essentially confirmed by Fässler and collaborators¹¹ in their independent density functional theory work using a different basis set. However, for M@Ge_{10}^{2-} with the larger interstitial palladium and platinum atoms, our work¹⁶ shows that the D_{5h} pentagonal prism is the lowest energy structure.¹⁶ For Pd@Ge_{10}^{2-} the D_{4d} bicapped square antiprism is found to lie ~ 13 kcal/mol in energy above the D_{5h} pentagonal prism. For Pt@Ge_{10}^{2-} with an even larger interstitial platinum atom, no low-energy D_{4d} bicapped square antiprismatic structure is even found.

The geometry of a regular pentagonal prism can be characterized by the ratio v/h between the lengths of the vertical edges shared by two rectangular faces (v) and the horizontal edges (h) of the pentagonal faces (Table 1). This v/h ratio is

Table 1. Dimensions of Pentagonal Prismatic Co@Ge_{10}^z Clusters^a

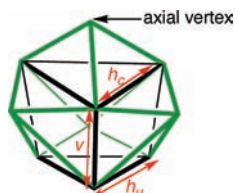


cluster	v	h	v/h
Co@Ge_{10} (19–2Q)	2.50	2.51	1.00
Co@Ge_{10} (19–3D)	2.51	2.51	1.00
Co@Ge_{10}^- (20–2T)	2.50	2.48	1.01
Co@Ge_{10}^- (20–3S)	2.50	2.47	1.01
Co@Ge_{10}^{2-} (21–2D)	2.54	2.48	1.02
Co@Ge_{10}^{3-} (22–2D)	2.59	2.50	1.03
Co@Ge_{10}^{3-} (expt.)	2.66	2.51	1.06
Co@Ge_{10}^{4-} (23–2D)	2.58	2.54	1.02
Co@Ge_{10}^{5-} (24–2D)	2.58	2.59	1.00

^aDistances in Å.

seen to be near unity for all of the low energy pentagonal prismatic Co@Ge_{10}^z structures ($z = 0$ to -5) having from 19 to 24 skeletal electrons. Thus the rectangular faces in all of these pentagonal prisms are squares or almost squares. The higher energy distorted Co@Ge_{10}^z structures **19–3D** (Figure 2) and **20–3S** (Figure 3) still recognizable as irregular pentagonal prisms are also included in Table 1. These structures represent lower spin state distorted versions of the regular pentagonal prismatic structures **19–2Q** and **20–2T**, where the distortion appears to be related to the Jahn–Teller effect. To determine effective v/h values for these distorted structures the non-equivalent vertical and horizontal edge lengths were first averaged to find effective values of v and h . These distorted pentagonal prismatic Co@Ge_{10}^z structures also have effective v/h ratios close to unity.

The other type of 10-vertex polyhedra found frequently in low-energy Co@Ge_{10}^z structures are polyhedra derived from the tetracapped trigonal prism (Figure 1). The four capping vertices in this polyhedron are of two types, namely, three vertices capping the three rectangular faces of the underlying trigonal prism and a fourth vertex capping one of the triangular

Table 2. Dimensions of Co@Ge₁₀^z Clusters with Ge₁₀ Polyhedra Derived from the Tetracapped Trigonal Prism^a

cluster	ν	h_c	h_u	Δh	\bar{h}	ν/\bar{h}	M@E ₁₀ distances
Co@Ge ₁₀ ⁺ (18–2S)	2.77	3.53	3.17	0.36	3.35	0.83	2.31(3),2.45(3),2.52(3),2.64(1)
Co@Ge ₁₀ (19–1D)	2.88	3.54	2.87	0.67	3.20	0.90	2.35(3),2.36(3),2.49(3),2.62(1)
Co@Ge ₁₀ ⁻ (20–1S)	2.99	3.62	2.67	0.95	3.14	0.95	2.35(3),2.40(3),2.42(3),2.44(1)
Ni@Ge ₁₀ (singlet)	3.00	3.62	2.70	0.92	3.16	0.95	2.36(3),2.41(3),2.43(3),2.46(1)
Ni@In ₁₀ ¹⁰⁻ (expt.)	~3.3	~4.3	~3.2	~1.1	~3.75	0.88	2.8(9),2.7(1)
Co@Ge ₁₀ ⁻ (20–4T)*	3.02	3.75	2.65	1.10	3.20	0.94	2.38(3),2.45(3),2.49(3),2.37(1)
Co@Ge ₁₀ ²⁻ (21–1D)*	3.02	3.69	2.73	0.96	3.21	0.94	2.38(3),2.40(3),2.44(3),2.47(1)
Co@Ge ₁₀ ²⁻ (21–3Q)	2.91	3.74	2.87	0.87	3.31	0.79	2.33(3),2.48(3),2.50(3),2.53(1)
Co@Ge ₁₀ ³⁻ (22–2T)	3.08	3.75	2.66	0.89	3.11	0.99	2.41(3),2.44(3),2.45(3),2.43(1)
Co@Ge ₁₀ ⁴⁻ (23–4Q)	3.31	3.56	2.62	0.94	3.09	1.07	2.39(3),2.44(3),2.47(3),2.83(1)
Co@Ge ₁₀ ⁵⁻ (24–3S)*	3.58	3.18	2.72	0.46	2.95	1.21	2.32(3),2.46(3),2.48(3),3.50(1)

^aDistances in Å. Structures distorted significantly from C_{3v} symmetry are starred.

faces of the underlying trigonal prism. This capping pattern reduces the D_{3h} symmetry of the underlying trigonal prism to C_{3v} symmetry. This symmetry point group partitions the ten vertices of the tetracapped trigonal prism into the following four sets:

- (1) The three vertices of the uncapped triangular face of the underlying trigonal prism;
- (2) The three vertices capping the rectangular faces of the underlying trigonal prism;
- (3) The three vertices of the capped triangular face of the underlying trigonal prism;
- (4) The unique vertex capping a triangular face of the underlying trigonal prism.

The edges of the tetracapped trigonal prism can be partitioned into six types. Three of these types of edges correspond to edges of the underlying trigonal prism whereas the other three types of edges are connected to the capping atoms. The edge lengths of the underlying trigonal prism can be used to characterize the geometries of the tetracapped trigonal prismatic structures encountered in this work. These edge lengths are as follows (Table 2):

- (1) The lengths ν of the vertical edges of the trigonal prism, i.e., the edges shared by two rectangular faces of the underlying trigonal prism;
- (2) The lengths h_c of the edges of the capped triangular face of the underlying trigonal prism;
- (3) The lengths h_u of the edges of the uncapped triangular face of the underlying trigonal prism.

Table 2 lists these edge lengths of the Co@Ge₁₀^z structures of C_{3v} symmetry derived from the tetracapped trigonal prism. In general the capping of only one of the two triangular faces makes the lengths h_c and h_u very different so that their difference $h_c - h_u = \Delta h$ can be used to measure the distortion of the underlying trigonal prism from its original D_{3h} symmetry to the C_{3v} structure with a cap at one end. The unique vertex capping the triangular face of the underlying trigonal prism is conveniently called the axial vertex in these structures since it is the only one of the ten vertices on the C₃ axis. Table 2 also lists the mean ν , h_c , and h_u edge lengths for Co@Ge₁₀^z structures

obviously derived from the C_{3v} tetracapped trigonal prism but distorted severely from ideal C_{3v} symmetry. These distorted structures are starred in Table 2.

An ideal C_{3v} tetracapped trigonal prism, like the D_{4d} bicapped square antiprism, is a deltahedron having 16 triangular faces (Figure 1). However, in ten-vertex germanium clusters two types of distortion of the ideal C_{3v} tetracapped trigonal prism are observed without breaking the C_{3v} symmetry. In such types of distortion one set of three symmetry-equivalent edges is elongated beyond “bonding distance” so that the resulting polyhedron is best considered having three quadrilateral faces and ten triangular faces. In the oblate or flattened C_{3v} polyhedra, which are exhibited by all of the lowest energy Co@Ge₁₀^z structures with C_{3v} symmetry, the axial vertex is pushed toward the center of the polyhedron. This brings all 10 germanium atoms within “bonding distance” of the cobalt atom, that is, less than 3.0 Å (typically less than 2.6 Å in most cases). This lengthens the edges of the capped triangular face of the underlying trigonal prism so that h_c becomes greater than 3.5 Å. The other possible C_{3v} polyhedron is the prolate or elongated polyhedron where the axial vertex remains beyond bonding distance to the central cobalt atom. In this case, the vertical edges of the underlying trigonal prism are elongated so that ν now becomes greater than 3.5 Å. The only Co@Ge₁₀^z structure of this type that was found in this work is the distorted Co@Ge₁₀⁵⁻ structure 24–3S, in which the average length of the vertical edges (ν) is 3.58 Å and the interstitial cobalt atom lies 3.50 Å from the axial germanium atom. Both the oblate and prolate C_{3v} polyhedral structures were found in a recent theoretical study³⁰ on the beryllium-centered cluster dianion Be@Ge₁₀²⁻.

The monoanion Co@Ge₁₀⁻ appears to be the species where C_{3v} geometry is the highly favored structure since the singlet 20–1S lies more than 16 kcal/mol in energy below any of the other Co@Ge₁₀⁻ structures found in this work (Figure 3). This monoanion is known only in the gas phase and has not been characterized structurally.^{17,18} However, this monoanion could arise from the two-electron oxidation of the known pentagonal prismatic trianion Co@Ge₁₀³⁻. Such an oxidation process would necessarily be a very delicate process since the cobalt

atoms in these clusters have a much lower formal oxidation state than in normal stable inorganic cobalt compounds so that “overoxidation” to cobalt(II) or even cobalt(III) is a distinct problem with most oxidizing agents. The rearrangement of the pentagonal prismatic structure of the trianion $\text{Co}@Ge_{10}^{3-}$ upon two-electron oxidation to the monoanion $\text{Co}@Ge_{10}^{-}$ is a distinct possibility since for the monoanion the C_{3v} polyhedral structure is predicted to lie 16.5 kcal/mol below the D_{5h} pentagonal prismatic structure. However, such a polyhedral rearrangement is predicted to require a change in spin state from the triplet pentagonal prismatic $\text{Co}@Ge_{10}^{-}$ (20–2T) to the singlet C_{3v} polyhedral $\text{Co}@Ge_{10}^{-}$ (20–1S).

The lowest-energy C_{3v} structure 20–1S predicted for the monoanion $\text{Co}@Ge_{10}^{-}$ can be related to theoretical and experimental studies on isoelectronic species. Thus the monoanion $\text{Co}@Ge_{10}^{-}$ is isoelectronic with neutral $\text{Ni}@Ge_{10}$, which is shown in previous theoretical work¹⁶ to have a C_{3v} global minimum. The values for v , h_o , h_w , Δh , \bar{h} , and v/\bar{h} as well as the 10 M–Ge distances for the isoelectronic species $\text{Co}@Ge_{10}^{-}$ and $\text{Ni}@Ge_{10}$ are essentially identical (within 0.03 Å and less in most cases). This comparison can be extended to the experimentally realized and structurally characterized species $\text{Ni}@In_{10}^{10-}$ found in the intermetallic $K_{10}In_{10}Ni$.²² The larger size of the indium atoms in $\text{Ni}@In_{10}^{10-}$ relative to the germanium atoms in $\text{Co}@Ge_{10}^{-}$ make the In–In and Ni–In distances in the former necessarily larger than the Ge–Ge and Co–Ge distances in the latter so that they are not necessarily directly comparable. However, the v/\bar{h} value of 0.88 found experimentally in $\text{Ni}@In_{10}^{10-}$ is reasonably close to the v/\bar{h} values of 0.95 predicted for both $\text{Co}@Ge_{10}^{-}$ and $\text{Ni}@Ge_{10}$ when the differences in cluster atoms, cluster environments, and cluster charges are considered.

5. SUMMARY

The lowest energy singlet $\text{Co}@Ge_{10}^z$ structures that are predicted to be particularly favorable energetically are the pentagonal prismatic $\text{Co}@Ge_{10}^{3-}$ trianion structure (22–1S in Figure 5) and the C_{3v} oblate polyhedral $\text{Co}@Ge_{10}^{-}$ monoanion structure derived from a tetracapped trigonal prism (20–1S in Figure 3). The pentagonal prismatic $\text{Co}@Ge_{10}^{3-}$ structure 22–1S has been realized experimentally in $[K(2,2,2\text{-crypt})]_4[\text{Co}@Ge_{10}][\text{Co}(1,5\text{-}C_8H_{12})_2] \cdot \text{toluene}$, characterized structurally by X-ray crystallography.¹¹ The C_{3v} polyhedral $\text{Co}@Ge_{10}^{-}$ structure has not been realized experimentally. However, analogous isoelectronic structures have been found theoretically¹⁶ for the neutral $\text{Ni}@Ge_{10}$ and experimentally²² for the $\text{Ni}@In_{10}^{10-}$ anion in the intermetallic $K_{10}In_{10}Ni$, characterized by X-ray crystallography.

The lowest energy structures for the remaining $\text{Co}@Ge_{10}^z$ species ($z = -5, -4, -2, 0$, and $+1$) are derived by addition or removal of electrons from these favorable $\text{Co}@Ge_{10}^{3-}$ and $\text{Co}@Ge_{10}^{-}$ structures. In general, these structures have one or more unpaired electrons. Thus low-energy pentagonal prismatic structures are found for $\text{Co}@Ge_{10}^z$ where $z = 0, -1, -2, -4$, and -5 with quartet, triplet, doublet, doublet, and triplet spin states, respectively. Similarly, low-energy C_{3v} polyhedral structures are found for $\text{Co}@Ge_{10}^z$ where $z = 0, -2, -3$, and -4 with doublet, doublet, triplet, and quartet spin states, respectively.

■ ASSOCIATED CONTENT

Supporting Information

Tables of distances; complete Gaussian reference (reference 28). This material is available free of charge via the Internet at <http://pubs.acs.org>.

■ AUTHOR INFORMATION

Corresponding Author

*E-mail: rbking@chem.uga.edu.

Notes

The authors declare no competing financial interest.

■ ACKNOWLEDGMENTS

This work was supported by CNCSIS-UEFISCSU, project number PNII-RU 465/2010, in Romania and by the National Science Foundation under Grants CHE-0716718 and CHE-1057466 in the U.S.A.

■ REFERENCES

- (1) Corbett, J. D. *Chem. Rev.* **1985**, *85*, 383.
- (2) Corbett, J. D. *Prog. Inorg. Chem.* **1976**, *21*, 129.
- (3) Williams, R. E. *Inorg. Chem.* **1971**, *10*, 210.
- (4) Wade, K. *Chem. Commun.* **1971**, 792.
- (5) Wade, K. *Adv. Inorg. Chem. Radiochem.* **1976**, *18*, 1.
- (6) Mingos, D. M. P. *Nat. Phys. Sci.* **1972**, *99*, 236.
- (7) Mingos, D. M. P. *Acc. Chem. Res.* **1984**, *17*, 311.
- (8) Schleyer, P. v. R.; Maerker, C.; Dransfeld, A.; Jiao, H.; van Eikema Hommes, N. J. R. *J. Am. Chem. Soc.* **1996**, *118*, 6317.
- (9) Schleyer, P. v. R.; Maerker, C.; Dransfeld, A.; Jiao, H.; van Eikema Hommes, N. J. R. *J. Am. Chem. Soc.* **1996**, *118*, 6317.
- (10) Chen, Z.; Neukemans, S.; Wang, X.; Janssens, E.; Zhou, Z.; Silverans, R. E.; King, R. B.; Schleyer, P. v. R.; Lievens, P. *J. Am. Chem. Soc.* **2006**, *128*, 12829.
- (11) Wang, J.-Q.; Stegmaier, S.; Fässler, T. F. *Angew Chem. Int. Ed.* **2009**, *48*, 1998.
- (12) Zhou, B.; Denning, M. S.; Kays, D. L.; Goicoechea, J. M. *J. Am. Chem. Soc.* **2009**, *132*, 2802.
- (13) Albano, V. G.; Demartin, F.; Iapalucci, M. C.; Longoni, G.; Sironi, A.; Zanotti, V. *Chem. Commun.* **1990**, 547.
- (14) King, R. B. *Dalton Trans.* **2004**, 3420.
- (15) King, R. B.; Silaghi-Dumitrescu, I.; Uță, M. M. *Inorg. Chem.* **2006**, *45*, 4974.
- (16) King, R. B.; Silaghi-Dumitrescu, I.; Uță, M. M. *J. Phys. Chem. A* **2009**, *113*, 527.
- (17) Zhang, X.; Li, G.; Gao, Z. *Rapid Commun. Mass Spectrom.* **2001**, *15*, 1573.
- (18) Li, G.; Zhang, X.; Tang, Z.; Gao, Z. *Chem. Phys. Lett.* **2002**, *359*, 203.
- (19) Sevov, S. C.; Corbett, J. C. *Inorg. Chem.* **1993**, *32*, 1059.
- (20) Esenturk, E. N.; Fettinger, J.; Eichhorn, B. *Chem. Commun.* **2005**, 247.
- (21) Esenturk, E. N.; Fettinger, J.; Eichhorn, B. *J. Am. Chem. Soc.* **2006**, *128*, 9178.
- (22) Henning, R. W.; Corbett, J. D. *Inorg. Chem.* **1999**, *38*, 3883.
- (23) Ruck, M.; Dubensky, V.; Söhnel, T. *Angew. Chem., Int. Ed.* **2003**, *45*, 2978.
- (24) Vosko, S. H.; Wilk, L.; Nusair, M. *Can. J. Phys.* **1980**, *58*, 1200.
- (25) Lee, C.; Yang, W.; Parr, R. G. *Phys. Rev. B* **1988**, *37*, 785.
- (26) Becke, A. D. *J. Chem. Phys.* **1993**, *98*, 5648.
- (27) Stephens, P. J.; Devlin, F. J.; Chabalowski, C. F.; Frisch, M. J. *J. Phys. Chem.* **1994**, *98*, 11623.
- (28) Frisch, M. J. et al. *Gaussian 09*, Revision A.02; Gaussian, Inc.: Wallingford, CT, 2009 (see Supporting Information for details).
- (29) Xie, Y.; Schaefer, H. F.; King, R. B. *J. Am. Chem. Soc.* **2000**, *122*, 8746.
- (30) King, R. B.; Silaghi-Dumitrescu, I.; Uță, M. M. *J. Phys. Chem. A* **2011**, *115*, 2847.